

## Conference Paper

# Bulk Oxygen Diffusion and Surface Exchange Limitations in $\text{La}_{2-x}\text{Sr}_x\text{Ni}_{1-y}\text{Fe}_y\text{O}_{4+\delta}$

A. R. Gilev, E. A. Kiselev, and V. A. Cherepanov

Department of Physical and Inorganic Chemistry, Institute of Natural Sciences and Mathematics, Ural Federal University, 620002 Ekaterinburg, Russia

## Abstract

The oxygen permeation flux through dense  $\text{La}_{1.2}\text{Sr}_{0.8}\text{Ni}_{0.9}\text{Fe}_{0.1}\text{O}_{4+\delta}$  membranes with different thicknesses (0.8 and 1.2 mm) was measured versus oxygen partial pressure gradient in the temperature range of 800–1000°C. The calculated values of critical membrane thickness clearly indicated the change of rate-limiting step from bulk oxygen diffusion ( $T < 900^\circ$ ) to surface exchange ( $T > 900^\circ$ ). In contrast to the promising cathode material, such as oxygen-excessive  $\text{La}_{1.5}\text{Sr}_{0.5}\text{Ni}_{0.6}\text{Fe}_{0.4}\text{O}_{4+\delta}$ , the oxygen-deficient  $\text{La}_{1.2}\text{Sr}_{0.8}\text{Ni}_{0.9}\text{Fe}_{0.1}\text{O}_{4+\delta}$  showed similar values of surface exchange coefficients, while oxygen-ion conductivity possessed higher activation energy and was significantly lower in the intermediate temperature range.

**Keywords:** lanthanum nickelate, membranes, oxygen diffusion, surface exchange

Corresponding Author:

A. R. Gilev  
artem.gilev@urfu.ru

Received: 14 September 2018

Accepted: 1 October 2018

Published: 14 October 2018

Publishing services provided by  
Knowledge E

© A. R. Gilev et al. This article is distributed under the terms of the Creative Commons

Attribution License, which permits unrestricted use and redistribution provided that the original author and source are credited.

Selection and Peer-review under the responsibility of the ASRTU Conference Committee.

## 1. Introduction

Impedance spectroscopy studies show that the  $\text{K}_2\text{NiF}_4$ -type  $\text{La}_2\text{NiO}_{4+\delta}$  is a promising cathode material for intermediate-temperature solid oxide fuel cells (IT-SOFCs) with a lower overpotential than that reported for  $\text{La}_{1-x}\text{Sr}_x\text{MnO}_{3-\delta}$  in the temperature range of 500–800°C [1]. With its total conductivity of  $\approx 80 \text{ S/cm}$  (at 400°C) and intermediate thermal expansion coefficient (TEC) values,  $\text{La}_2\text{NiO}_{4+\delta}$  exhibited similar oxygen diffusion compared with that for  $\text{La}_{0.8}\text{Sr}_{0.1}\text{Ga}_{0.8}\text{Mg}_{0.2}\text{O}_3$  and  $\text{La}_{0.6}\text{Sr}_{0.4}\text{Co}_{0.2}\text{Fe}_{0.8}\text{O}_3$  [2]. However, Skinner et al. reported that the activation energy of surface exchange in  $\text{La}_2\text{NiO}_{4+\delta}$  and  $\text{La}_{1.9}\text{Sr}_{0.1}\text{NiO}_{4+\delta}$  was approximately twice higher compared to the diffusion process [2]. The surface exchange limitations in  $\text{La}_2\text{NiO}_{4+\delta}$  were evidenced by oxygen permeation studies [3]: the maximal fluxes were obtained for the tape-casted 3-layer  $\text{La}_2\text{NiO}_{4+\delta}$  membranes with porous layers on both sides.

## OPEN ACCESS

The A- and B-site doping of  $\text{La}_2\text{NiO}_{4+\delta}$  was shown to affect its properties, including oxygen diffusion and oxygen surface exchange [2, 4–8]. In general, acceptor-type A-site doping leads to a decrease in oxygen over-stoichiometry and an increase in electron hole transport due to partial oxidation of  $\text{Ni}^{2+}$  to  $\text{Ni}^{3+}$  [4]. The A-site substitution in the range of  $x = 0\text{--}0.4$  in  $\text{La}_{2-x}\text{A}_x\text{NiO}_{4+\delta}$  ( $\text{A} = \text{Ca}, \text{Sr}$ ) drastically decreases oxygen-ion conductivity and slightly improves the surface exchange kinetics [6] resulting in inferior electrochemical properties of  $\text{La}_{2-x}\text{A}_x\text{NiO}_{4+\delta}$  compared to the undoped  $\text{La}_2\text{NiO}_{4+\delta}$  [9]. The B-site substitution with donor-type dopants, such as Fe or Co, qualitatively produces the opposite effect on the properties of  $\text{La}_2\text{NiO}_{4+\delta}$  compared with that for the Ca/Sr doping [5]. Introduction of these dopants does not have a significant effect on the oxygen-ion conductivity, although the surface exchange kinetics of oxygen is noticeably improved [7, 8].

As shown for  $\text{La}_{2-x}\text{Sr}_x\text{Ni}_{1-y}\text{Fe}_y\text{O}_{4+\delta}$ , the simultaneous doping with strontium and iron eliminates the surface oxygen exchange limitations at  $x = 0.5$ ,  $y = 0.4$  [10] improving its performance as a cathode material for SOFCs [11]. Taking into account the recent results reported in [12], where an increase in strontium content from  $x = 0.2$  to  $x = 0.8$  in  $\text{La}_{2-x}\text{Sr}_x\text{NiO}_{4+\delta}$  decreased the area-specific resistance (ASR) of a symmetrical cell based on the  $\text{Ce}_{0.8}\text{Sm}_{0.2}\text{O}_{1.9}$  substrate almost fourfold (from  $0.41$  to  $0.12 \text{ } \Omega/\text{cm}^2$  at  $800^\circ\text{C}$ ), it is interesting to study bulk oxygen diffusion and surface oxygen exchange limitations in  $\text{La}_{1.2}\text{Sr}_{0.8}\text{Ni}_{0.9}\text{Fe}_{0.1}\text{O}_{4+\delta}$  and compare it with the studied earlier oxygen-excessive  $\text{La}_{1.5}\text{Sr}_{0.5}\text{Ni}_{1-y}\text{Fe}_y\text{O}_{4+\delta}$  ( $y = 0.1, 0.3$ , and  $0.4$ ) oxides [10].

## 2. Methods

The  $\text{La}_{1.2}\text{Sr}_{0.8}\text{Ni}_{0.9}\text{Fe}_{0.1}\text{O}_{4+\delta}$  complex oxide was synthesized by a citrate-nitrate technique using the following starting materials:  $\text{La}(\text{NO}_3)_3 \cdot 6\text{H}_2\text{O}$  ( $> 99\%$ ),  $\text{SrCO}_3$  ( $\geq 99.9\%$ ),  $\text{FeC}_2\text{O}_4 \cdot 2\text{H}_2\text{O}$  ( $\geq 99.9\%$ ),  $\text{Ni}(\text{CH}_3\text{COO})_2 \cdot 4\text{H}_2\text{O}$  ( $99\%$ ),  $\text{C}_6\text{H}_8\text{O}_7 \cdot \text{H}_2\text{O}$  ( $99\%$ ), and  $\text{HNO}_3$  ( $65\%$ ,  $\geq 99.9\%$ ). The synthesis procedure can be found in [10]. The obtained powders were uniaxially pressed into pellets ( $15 \text{ mm}$  in diameter) and sintered at  $1320^\circ\text{C}$  for  $20 \text{ h}$  in air yielding relative density of  $\geq 95\%$ . The X-ray powder diffraction performed at room temperature (using an Equinox 3000 instrument,  $\text{Cu-K}_\alpha$  radiation) revealed phase purity of the  $\text{La}_{1.2}\text{Sr}_{0.8}\text{Ni}_{0.9}\text{Fe}_{0.1}\text{O}_{4+\delta}$  membranes. The sintered pellets were mechanically polished to obtain the necessary thicknesses of  $0.8$  and  $1.2 \text{ mm}$ .

The preparation of cell for oxygen permeation studies and the experimental details were described in [10]. The data were collected at  $800, 850, 900, 950$ , and  $1000^\circ\text{C}$

in the oxygen partial pressure ( $p_{O_2}$ ) gradient interval of  $\log(0.21/p_{O_2}) = 0.2\text{--}1.8$ . The experiment with the 0.8 mm thick membrane was carried out twice to evaluate the reproducibility of the obtained results.

### 3. Results

The steady-state oxygen permeation fluxes ( $j$ ) through the dense  $\text{La}_{1.2}\text{Sr}_{0.8}\text{Ni}_{0.9}\text{Fe}_{0.1}\text{O}_{4+\delta}$  membranes with 0.8 and 1.2 mm thickness are shown in Figure 1(a) as a function of  $p_{O_2}$  gradient. As can be seen from Figure 1(a), the results of two parallel experiments with the 0.8 mm thick membrane illustrate good reproducibility. Figure 1(b) shows the specific oxygen permeability ( $J$ ) that was calculated as follows:

$$J = j \times d \times \left[ \ln \frac{0.21}{p_{O_2}} \right]^{-1}, \quad (1)$$

where  $d$  is a membrane thickness.

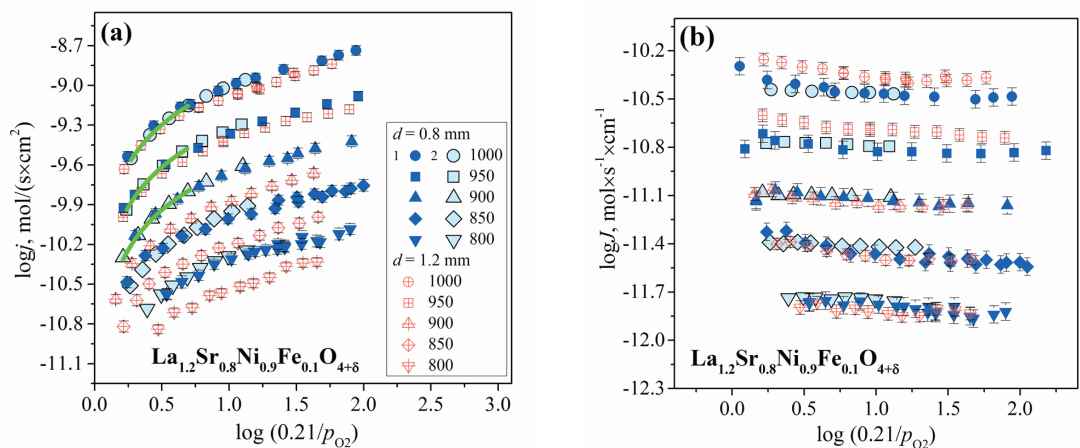


**Figure 1:** Steady-state oxygen permeation flux (a) and specific oxygen permeability (b) through dense 0.8- and 1.2-mm thick membranes  $\text{La}_{1.2}\text{Sr}_{0.8}\text{Ni}_{0.9}\text{Fe}_{0.1}\text{O}_{4+\delta}$  versus oxygen partial pressure gradient at different temperatures.

According to Eq. (1) the specific oxygen permeability, which is proportional to the  $j \times d$  product, will not depend on membrane thickness, if the oxygen permeation flux through a dense membrane is limited by bulk oxygen diffusion. As can be seen from Figure 1(b), the obtained  $J$  values were independent of the membrane thickness within the experimental error at 800, 850, and 900 °C. However, at 950 and 1000 °C a notable gain in permeability with increase in membrane thickness can be observed indicating significant surface exchange limitations [5].

In order to assess the role of bulk diffusion and surface exchange in the oxygen permeation flux, the critical membrane thickness ( $d_c$ ) can be calculated. The  $d_c$  value

corresponds to the change of rate-limiting step from surface exchange to bulk diffusion (with increase in a membrane thickness) at fixed temperature and  $p_{O_2}$  gradient. It can be evaluated by the modified Wagner equation, which can be presented as follows [10]:

$$\frac{1}{j} \ln \left( \frac{p_2}{p_1} \right) = \frac{16F^2 d}{RT\sigma_{amb}} + [k_{ex1}]^{-1} + [k_{ex2}]^{-1} = \frac{16F^2(d + d_c)}{RT\sigma_{amb}}, \quad (2)$$

where  $p_2$  ( $= 0.21$  atm),  $k_{ex1}$  and  $p_1$  ( $= p_{O_2}$ ),  $k_{ex2}$  denote the oxygen partial pressure and surface exchange coefficient at the feed- and permeate-side of a membrane, respectively;  $\sigma_{amb}$  stands for ambipolar conductivity.

The critical membrane thickness, ambipolar conductivity, and the sum  $[k_{ex1}]^{-1} + [k_{ex2}]^{-1}$  as functions of  $p_{O_2}$  gradient were calculated using Eq. (2) as described in [10]. Figure 2(a) shows the obtained  $d_c = f(\log(0.21/p_{O_2}))$  dependencies. The critical membrane thickness was lower than 0.8 mm in the temperature range of 800–900°C, but it noticeably increased at 950 and 1000°C reaching values higher than 1.2 mm. Such behavior of  $d_c$  clearly indicated the change of rate-limiting step from bulk diffusion to surface exchange in the temperature range of 900–950°C. One should note that the change of rate-limiting step correlated with the beginning of active oxygen release from the  $\text{La}_{1.2}\text{Sr}_{0.8}\text{Ni}_{0.9}\text{Fe}_{0.1}\text{O}_{4+\delta}$  sample (at  $T > 900^\circ\text{C}$ ) followed by a reduction of  $\text{Ni}^{3+}$  to  $\text{Ni}^{2+}$  and formation of oxygen vacancies [13]. The latter observation hints that  $\text{Ni}^{3+}/\text{Ni}^{2+}$  ratio may affect the surface exchange in  $\text{La}_{1.2}\text{Sr}_{0.8}\text{Ni}_{0.9}\text{Fe}_{0.1}\text{O}_{4+\delta}$ .

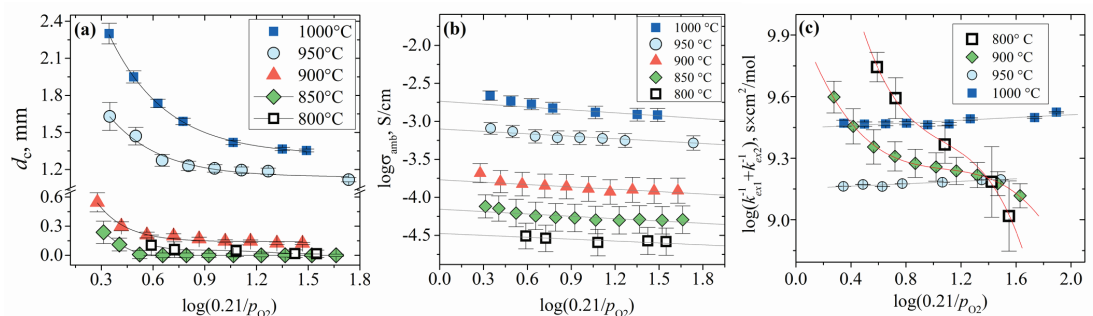


**Figure 2:** Critical membrane thickness (a), ambipolar conductivity (b), and sum of reverse surface exchange coefficients (c) for  $\text{La}_{1.2}\text{Sr}_{0.8}\text{Ni}_{0.9}\text{Fe}_{0.1}\text{O}_{4+\delta}$  versus oxygen partial pressure gradient at different temperatures.

The calculated values of ambipolar conductivity and the sum of reverse exchange constants  $[k_{ex1}]^{-1} + [k_{ex2}]^{-1}$  are shown in Figures 2(b) and 2(c), respectively. As can be seen from Figure 2(b), the ambipolar conductivity possessed a relatively weak dependency versus  $p_{O_2}$  gradient showing a minor decrease in the range of  $0.3 \leq \log(0.21/p_{O_2}) \leq 0.6$ . The latter fact allowed defining the  $\sigma_{amb}$  values in air by extrapolating the corresponding dependencies to zero  $p_{O_2}$  gradient (Figure 2(b)). One should note that the  $\sigma_{amb}$  values are approximately equal to the bulk oxygen-ion conductivity

in  $\text{La}_{2-x}\text{Sr}_x\text{Ni}_{1-y}\text{Fe}_y\text{O}_{4+\delta}$  according to our previous studies [10, 14]. Furthermore, the oxygen diffusion coefficients can be calculated using the obtained values of oxygen-ion conductivity and the data on oxygen non-stoichiometry from [14] by the Nernst-Einstein equation as it was performed in [10].

The reciprocal temperature dependencies of oxygen-ion conductivity ( $\sigma_o$ ) and oxygen diffusion coefficients ( $D$ ) for  $\text{La}_{1.2}\text{Sr}_{0.8}\text{Ni}_{0.9}\text{Fe}_{0.1}\text{O}_{4+\delta}$  in air are plotted in Figures 3(a) and 3(b), respectively, together with the data for the oxygen-excessive  $\text{La}_{1.5}\text{Sr}_{0.5}\text{Ni}_{1-y}\text{Fe}_y\text{O}_{4+\delta}$  oxides reported earlier in [10]. As can be seen from Figures 3(a) and 3(b),  $\text{La}_{1.2}\text{Sr}_{0.8}\text{Ni}_{0.9}\text{Fe}_{0.1}\text{O}_{4+\delta}$  and  $\text{La}_{1.5}\text{Sr}_{0.5}\text{Ni}_{1-y}\text{Fe}_y\text{O}_{4+\delta}$  showed comparable values of oxygen diffusion coefficients at all studied temperatures, while oxygen-ion conductivity in the former was lower in the 800–900°C temperature interval. Both,  $\sigma_o$  and  $D$  in oxygen-deficient  $\text{La}_{1.2}\text{Sr}_{0.8}\text{Ni}_{0.9}\text{Fe}_{0.1}\text{O}_{4+\delta}$  showed higher activation energies compared to that for oxygen-excessive  $\text{La}_{1.5}\text{Sr}_{0.5}\text{Ni}_{1-y}\text{Fe}_y\text{O}_{4+\delta}$ .

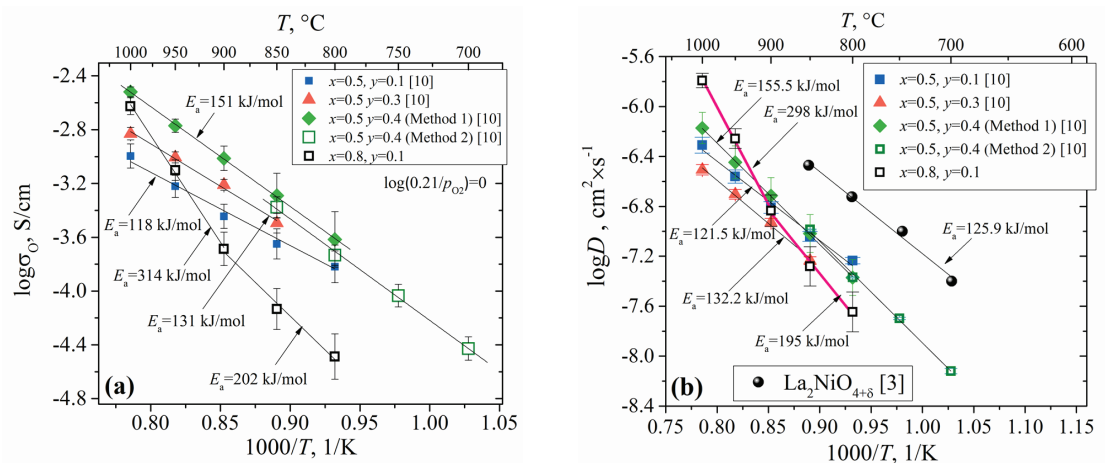


**Figure 3:** Reciprocal temperature dependencies of oxygen-ion conductivity (a) and oxygen diffusion coefficients (b) for  $\text{La}_{1.2}\text{Sr}_{0.8}\text{Ni}_{0.9}\text{Fe}_{0.1}\text{O}_{4+\delta}$  in air (the details on Methods 1 and 2 can be found in Reference [10]).

The surface oxygen exchange coefficients in air can be estimated if one assumes that at low  $p_{\text{O}_2}$  gradients  $k_{\text{ex}1}$  and  $k_{\text{ex}2}$  are approximately equal and, hence, the  $k_{\text{ex}}$  value can be easily found from the corresponding sum  $[k_{\text{ex}1}]^{-1} + [k_{\text{ex}2}]^{-1}$ . The latter can be determined as a fitting parameter in the model function, Eq. (2), presented in the form of  $\log j = f(\ln(p_2/p_1))$ , where  $\sigma_{\text{amb}} \approx \sigma_o$  is the extrapolated value at a given temperature. In this case, the sum  $[k_{\text{ex}1}]^{-1} + [k_{\text{ex}2}]^{-1}$  should be constant or vary insignificantly in the given range of  $p_{\text{O}_2}$  gradients. For  $\text{La}_{1.2}\text{Sr}_{0.8}\text{Ni}_{0.9}\text{Fe}_{0.1}\text{O}_{4+\delta}$ , this is achieved only at relatively low  $p_{\text{O}_2}$  gradients in the temperature range of 900–1000°C (Figure 2(c)). Therefore, the model function was fitted to the experimental oxygen permeation fluxes in the range of  $\log(0.21/p_{\text{O}_2}) = 0.2\text{--}0.6$  at 900, 950, and 1000°C. The results are shown in Figure 1(a) by the solid green lines indicating good agreement with the

experimental data. Similarly, the  $k_{ex}$  values were estimated for  $\text{La}_{1.5}\text{Sr}_{0.5}\text{Ni}_{1-y}\text{Fe}_y\text{O}_{4+\delta}$  using the data from [10]. As can be seen from Figure 4, the activation energy for surface exchange in  $\text{La}_{1.2}\text{Sr}_{0.8}\text{Ni}_{0.9}\text{Fe}_{0.1}\text{O}_{4+\delta}$  was almost twice lower compared to that for the oxygen-excessive  $\text{La}_{1.5}\text{Sr}_{0.5}\text{Ni}_{1-y}\text{Fe}_y\text{O}_{4+\delta}$  oxides. The obtained results also indicated that the surface oxygen exchange kinetics for  $\text{La}_{1.2}\text{Sr}_{0.8}\text{Ni}_{0.9}\text{Fe}_{0.1}\text{O}_{4+\delta}$  should be similar to  $\text{La}_{1.5}\text{Sr}_{0.5}\text{Ni}_{0.6}\text{Fe}_{0.4}\text{O}_{4+\delta}$  in the intermediate temperature range (see the dashed lines in Figure 4).

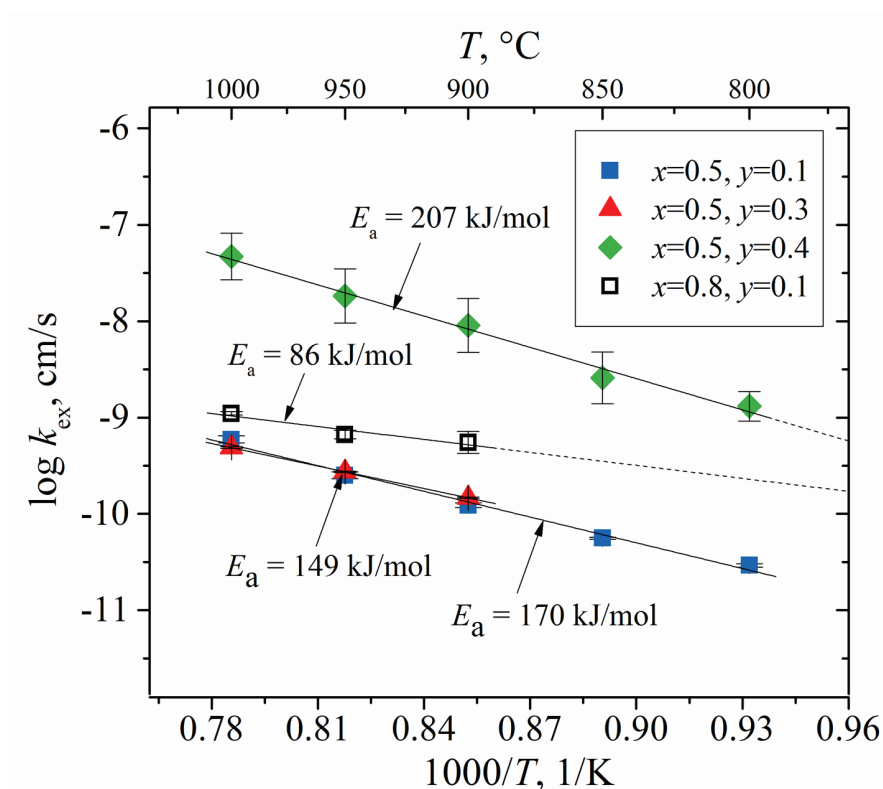


**Figure 4:** Surface exchange coefficients versus temperature for  $\text{La}_{2-x}\text{Sr}_x\text{Ni}_{1-y}\text{Fe}_y\text{O}_{4+\delta}$ .

## 4. Conclusion

The studies of oxygen permeation flux through dense  $\text{La}_{1.2}\text{Sr}_{0.8}\text{Ni}_{0.9}\text{Fe}_{0.1}\text{O}_{4+\delta}$  membranes with different thicknesses (0.8 and 1.2 mm) allowed calculating the critical membrane thickness. The obtained values indicated significant surface limitations in the oxide at 950 and 1000°C. The latter induced the change of rate-limiting step from bulk diffusion (800–900°C) to surface exchange (900–1000°C) upon temperature increase. The values of oxygen diffusion coefficients for  $\text{La}_{1.2}\text{Sr}_{0.8}\text{Ni}_{0.9}\text{Fe}_{0.1}\text{O}_{4+\delta}$  were comparable with that obtained earlier for oxygen-excessive  $\text{La}_{1.5}\text{Sr}_{0.5}\text{Ni}_{1-y}\text{Fe}_y\text{O}_{4+\delta}$  at all studied temperatures, while the oxygen-ion conductivity was lower by almost one

order in magnitude at 800 and 850°C. The calculated values of surface exchange coefficients showed that increase in strontium content from  $x = 0.5$  to  $0.8$  reduced the activation energy of surface exchange almost twice leading to a similar surface exchange kinetics in  $\text{La}_{1.2}\text{Sr}_{0.8}\text{Ni}_{0.9}\text{Fe}_{0.1}\text{O}_{4+\delta}$  and  $\text{La}_{1.5}\text{Sr}_{0.5}\text{Ni}_{0.6}\text{Fe}_{0.4}\text{O}_{4+\delta}$  in the intermediate temperature range. One can conclude that  $\text{La}_{1.5}\text{Sr}_{0.5}\text{Ni}_{0.6}\text{Fe}_{0.4}\text{O}_{4+\delta}$  should be considered as a superior cathode material compared to the strontium-rich  $\text{La}_{1.2}\text{Sr}_{0.8}\text{Ni}_{0.9}\text{Fe}_{0.1}\text{O}_{4+\delta}$ : although both exhibited comparable surface exchange kinetics the latter showed significantly lower oxygen-ion conductivity values in the intermediate temperature range.

## Acknowledgements

The authors would like to acknowledge that the equipment of the Ural Center for Shared Use 'Modern nanotechnology' SNSM UrFU was used in this research.

## Funding

The research was supported by the Ministry of Education and Science of the Russian Federation Agreement No. 02.A03.21.0006.

## References

- [1] Mauvy, F., Lalanne, C., Bassat, J. M., et al. (2005). Oxygen reduction on porous  $\text{Ln}_2\text{NiO}_{4+\delta}$  electrodes. *Journal of the European Ceramic Society*, vol. 25, pp. 2669–2672.
- [2] Skinner, S. J. and Kilner, J. A. (2000). Oxygen diffusion and surface exchange in  $\text{La}_{2-x}\text{Sr}_x\text{NiO}_{4+\delta}$ . *Solid State Ionics*, vol. 135, pp. 709–712.
- [3] Shaula, A. L., Naumovich, E. N., Viskup, A. P., et al. (2009). Oxygen transport in  $\text{La}_2\text{NiO}_{4+\delta}$ : Assessment of surface limitations and multilayer membrane architectures. *Solid State Ionics*, vol. 180, pp. 812–816.
- [4] Tang, J. P., Dass, R. I., and Manthiram, A. (2000). Comparison of the crystal chemistry and electrical properties of  $\text{La}_{2-x}\text{A}_x\text{NiO}_4$  ( $\text{A} = \text{Ca}, \text{Sr}, \text{and Ba}$ ). *Materials Research Bulletin*, vol. 35, pp. 411–424.
- [5] Kharton, V. V., Tsipis, E. V., Naumovich, E. N., et al. (2008). Mixed conductivity, oxygen permeability and redox behavior of  $\text{K}_2\text{NiF}_4$ -type  $\text{La}_2\text{Ni}_{0.9}\text{Fe}_{0.1}\text{O}_{4+\delta}$ . *Journal of Solid State Chemistry*, vol. 181, pp. 1425–1433.



- [6] Li, Z., Haugsrud, R., and Norby, T. (2011). Oxygen bulk diffusion and surface exchange in Sr-substituted  $\text{La}_2\text{NiO}_{4+\delta}$ . *Solid State Ionics*, vol. 184, pp. 42–46.
- [7] Klande, T., Efimov, K., Cusenza, S., et al. (2011). Effect of doping, microstructure, and  $\text{CO}_2$  on  $\text{La}_2\text{NiO}_{4+\delta}$ -based oxygen-transporting materials. *Journal of Solid State Chemistry*, vol. 184, pp. 3310–3318.
- [8] Kilner, J. A. and Shaw, C. K. M. (2002). Mass transport in  $\text{La}_2\text{Ni}_{1-x}\text{Co}_x\text{O}_{4+\delta}$  oxides with the  $\text{K}_2\text{NiF}_4$  structure. *Solid State Ionics*, vol. 154–155, pp. 523–527.
- [9] Pikalova, E. Yu., Bogdanovich, N. M., Kolchugin, A. A., et al. (2014). Electrical and electrochemical properties of  $\text{La}_2\text{NiO}_{4+\delta}$ -based cathodes in contact with  $\text{Ce}_{0.8}\text{Sm}_{0.2}\text{O}_{2-\delta}$  electrolyte. *Procedia Engineering*, vol. 98, pp. 105–110.
- [10] Gilev, A. R., Kiselev, E. A., and Cherepanov, V. A. (2018). Oxygen transport phenomena in  $(\text{La},\text{Sr})_2(\text{Ni},\text{Fe})\text{O}_4$  materials. *Journal of Materials Chemistry A*, vol. 6, pp. 5304–5312.
- [11] Gilev, A. R., Kiselev, E. A., and Cherepanov, V. A. (2016). Strontium and iron substituted lanthanum nickelate as cathode material in solid oxide fuel cells. *IV Sino-Russian ASRTU Symposium on Advanced Materials and Materials and Processing Technology, KnE Materials Science*, pp. 64–70.
- [12] Wang, Y. P., Xu, Q., Huang, D. P., et al. (2017). Survey on electrochemical properties of  $\text{La}_{2-x}\text{Sr}_x\text{NiO}_{4\pm\delta}$  ( $x=0.2$  and  $0.8$ ,  $\delta > 0$ ) cathodes related with structural stability under cathodic polarization conditions. *International Journal of Hydrogen Energy*, vol. 42, pp. 6290–6302.
- [13] Gilev, A. R., Kiselev, E. A., Zakharov, D. M., et al. (2017). Interrelation of transport properties, defect structure and spin state of  $\text{Ni}^{3+}$  in  $\text{La}_{1.2}\text{Sr}_{0.8}\text{Ni}_{0.9}\text{Fe}_{0.1}\text{O}_{4+\delta}$ . *Solid State Sciences*, vol. 72, pp. 134–143.
- [14] Gilev, A. R., Kiselev, E. A., and Cherepanov, V. A. (2016). Homogeneity range, oxygen nonstoichiometry, thermal expansion and transport properties of  $\text{La}_{2-x}\text{Sr}_x\text{Ni}_{1-y}\text{Fe}_y\text{O}_{4+\delta}$ . *RSC Advances*, vol. 6, pp. 72905–72917.